

Synergistic roles of carbon fibres and ZrO_2 particles in strengthening and toughening Li- α -sialon composites

Z.B. Yu^a, D.P. Thompson^{a,*}, A.R. Bhatti^b

^aMaterials Division, Department of Mechanical, Materials and Manufacturing Engineering, University of Newcastle upon Tyne, NE1 7RU, UK

^bStructural Materials Centre, DERA Farnborough, Hampshire GU14 0XL, UK

Received 2 November 2000; received in revised form 8 March 2001; accepted 24 March 2001

Abstract

Carbon fibre reinforced Li- α -sialon ceramic matrix composites have been fabricated by a process of slurry infiltration followed by hot-pressing. The roles of both carbon fibres and ZrO_2 particles in the strengthening and toughening of Li- α -sialon ceramic matrix composites are discussed. SEM observations show that microcracks in the matrix resulting from the thermal mismatch between the carbon fibres and the matrix can be eliminated by the addition of the ZrO_2 and a considerable amount of fibre pullout was achieved during fracture failure of the composites. Measurement of mechanical properties indicates that a synergistic strengthening and toughening has been achieved with bending strength and fracture toughness of ~ 410 MPa and ~ 12 MPa $\text{m}^{1/2}$ respectively. © 2001 Elsevier Science Ltd. All rights reserved.

Keywords: Carbon fibre; Composites; Mechanical properties; Reinforcement; Sialon; Particles

1. Introduction

Carbon fibres have been extensively used to reinforce glass, glass-ceramic, and ceramic-matrix composites because they offer an excellent combination of strength, modulus, and toughness,^{1–5} and of the available fibres, they retain their mechanical properties most successfully above 1000°C. However, carbon fibres have a high thermal anisotropy, and for example, the thermal expansion coefficients are $(0.67–1.0) \times 10^{-6} \text{ }^\circ\text{C}^{-1}$ and $(8–27) \times 10^{-6} \text{ }^\circ\text{C}^{-1}$ in the axial and radial directions respectively.^{3,6} This anisotropy makes it rather difficult for carbon fibres to be compatible with most other matrices in both directions simultaneously. To solve this problem, the most common procedure is to adjust the thermal expansion coefficient of the matrix, and for example in carbon fibre reinforced $\text{Li}_2\text{O}-\text{Al}_2\text{O}_3-\text{SiO}_2$ (LAS) matrix composites, glasses with aluminium-rich compositions have a low thermal expansion coefficient $(0–12) \times 10^{-7} \text{ }^\circ\text{C}^{-1}$,⁷ which can be easily increased just by adding other cations. However, in the carbon fibre/nitrogen

glass system, and especially the rare earth sialon glass system, although the glass forming regions in these systems are also extensive and the thermal expansion coefficient can be adjusted significantly, it is still difficult to achieve low enough values to be compatible with the carbon fibre axial direction.⁸ As for carbon fibre/ceramic systems, the scope for adjustment of the thermal expansion coefficient in a single-phase ceramic is very limited once the overall chemical composition is determined. Therefore transverse cracks perpendicular to the carbon fibre axial direction forming after preparation have been reported in these materials.^{3,4,9}

Another possible way is to incorporate particles of ZrO_2 into the matrix so that the thermal expansion behaviour of the matrix can be changed by the $t \rightarrow m$ - ZrO_2 transformation. This method is not suitable for glasses with T_g lower than the $t \rightarrow m$ transformation temperature ($\sim 1170^\circ\text{C}$) because the volume change from the transformation is absorbed by plastic deformation. It has been reported that additions of ZrO_2 to silicon nitride³ and nitrogen glasses⁴ can eliminate the micro-cracks caused by the thermal mismatch.

In this paper, carbon fibre reinforced Li- α -sialon composites have been prepared and the effect of processing parameters on the mechanical properties and

* Corresponding author. Tel.: +44-191-2227202; fax: +44-191-2227153.

E-mail address: d.p.thompson@newcastle.ac.uk (D.P. Thompson).

fracture behaviour of the composites examined; the formation of microcracks in the matrix has been analysed. The use of carbon fibres and monoclinic ZrO_2 particles together for the reinforcement of Li- α -sialon ceramics has been explored based on the following considerations: (1) the incorporation of carbon fibres is expected to improve the fracture toughness, and the mode of fracture, and hence to increase the damage tolerance of the composites; and (2) the addition of monoclinic ZrO_2 particles should alleviate the stresses generated by matrix contraction, thereby removing the micro-cracks resulting from the thermal mismatch between the fibres and the matrix. By a combination of these two effects, it was expected that both strengthening and toughening could be achieved simultaneously. The transformability of ZrO_2 and its chemical compatibility with the matrix are discussed.

2. Experimental procedure

2.1. Synthesis of pure Li- α -sialon

An $m=1.3$, $n=1.2$ α -sialon, of general formula $\text{M}_x\text{Si}_{12-(m+n)}\text{Al}_{(m+n)}\text{O}_n\text{N}_{16-n}$, was chosen for the overall composition because this composition is located fairly centrally within the single-phase α -sialon region on the α -sialon plane, and can be prepared in high purity. Si_3N_4 (H.C. Starck, G10), AlN (H.C. Starck, grade B), Li_2CO_3 (BDH, 99%) and SiO_2 (BDH, precipitated) were employed as starting materials; the process of mixing, and drying remained as reported in a previous paper.⁹ A mixture of 50 wt.% BN and 50 wt.% $\text{Li}_2\text{CO}_3/\text{AlN}/\text{Si}_3\text{N}_4$ powder was chosen as the packing powder to retard the volatilisation of gaseous Li species. The pre-shaped $\Phi 40 \times 20$ mm green body was pressureless sintered in an inductively-heated graphite furnace under a N_2 atmosphere at 1700°C for 1 h.

2.2. LAS glass powder preparation

LAS glass of composition $\text{Li}_{40}\text{Al}_6\text{Si}_{60}\text{O}_{149}$ was chosen as the sintering additive, because (1) LAS glasses were reported to have good chemical compatibility with carbon fibres,^{10,11} thus some chemical reactions between carbon fibres and the matrix can be avoided at relatively low sintering temperatures, (2) this composition has a low eutectic temperature ($\sim 1050^\circ\text{C}$) according to the $\text{Li}_2\text{O}-\text{Al}_2\text{O}_3-\text{SiO}_2$ phase diagram¹² and (3) it was expected that Li- α -sialon would partially dissolve in the LAS glass thus facilitating sintering of the composite.

LAS glass was prepared by melting the batch compounds Li_2CO_3 , SiO_2 and Al_2O_3 in a graphite crucible at 1250 – 1300°C for 30 min in a N_2 atmosphere and then fast cooling to room temperature.

The bulk Li- α -sialon and LAS glass were crushed and ground to a fine particle size for later use.

2.3. Composite fabrication and characterization

The as-prepared Li- α -sialon powder, LAS glass powder and ZrO_2 powder (TOSOH, TZ-0, see Table 1) were mixed together by ball milling for 60 h using sialon balls in iso-propanol in a rubber cylinder. The resulting slurry was then dried using an infra-red lamp. The mixed and milled powders were mixed in a PVA water solution containing 3–5 wt.% of PVA, and stirred ultrasonically to form a homogeneous slurry. Carbon fibre tows (Toraca, Grade X555, see Table 2) were fed carefully through the slurry tank containing the as-formed slurry. The slurry-impregnated carbon fibre tows were wound on to a drum in an aligned arrangement, and after partial drying, cut into short segments and 1D stacked for cold pressing. The completely dried green bodies were hot-pressed under different conditions. Fig. 1 schematically shows the processes used for slurry formation and composite fabrication.

Fibre volume fraction measurement was carried out by using the ‘washing out’ method.⁴ After hot-pressing, density measurements were carried out by of mercury displacement, phases were analysed by X-ray powder diffraction using a Hägg–Guinier X-ray focusing camera. Samples were machined and polished to $3 \times 4 \times 45$ mm for strength testing and $2 \times 4 \times 45$ mm for fracture toughness measurement. Generally tensile testing is more appropriate, but in the present paper, bend testing, which is very commonly used for ceramic materials, was chosen because the preparation and machining of ceramic samples is much easier and cheaper. The three-point bend test was carried out on an INSTRON machine, with a span of 30 mm, and a load rate of 0.2

Table 1
Properties of TOSOH TZ-0 zirconia powder

Chemical analysis	Al_2O_3	<0.005 wt. %
	SiO_2	0.007 wt. %
	Fe_2O_3	<0.002 wt. %
	Na_2O	0.020 wt. %
	Ig loss	0.78 wt. %
Crystallite size		27 nm
Specific surface area		15.3 m ² /g

Table 2
Properties of TORAYCA (Grade X555) carbon fibres

Filament no.	12,000 Filaments per tow
Diameter	5–6 μm
Density	1.80 g/cm ³
Young's modulus	257 GPa
Tensile strength	4470 MPa
TEC ^a (in axis direction) α_a	$(0.67\text{--}1.0) \times 10^{-6} ^\circ\text{C}^{-1}$
TEC ^a (in radial direction) α_r	$(8\text{--}27) \times 10^{-6} ^\circ\text{C}^{-1}$

^a TEC, thermal expansion coefficient.^{3,6}

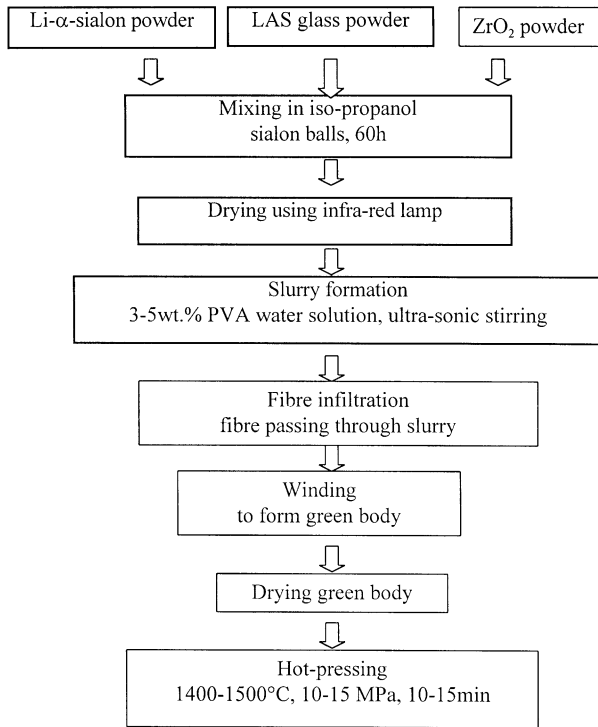


Fig. 1. Schematic representation of slurry formation and composite fabrication.

mm/min. The distribution of carbon fibres in the composites and microstructure of fracture surfaces of the composites after bend testing were observed using a HITACHI S-2400 Scanning Electron Microscope; Young's moduli for composite samples were determined by four-point bending using bar shaped specimens (3×4×45 mm). Two strain gauges, which were attached to the upper and lower sides of each specimen to offset the disturbance arising from the unevenness of the specimen, were connected to the strain indicator (Model P-350A, RALEIGH, North Carolina) to measure the strain changes during the test. The stress can be obtained directly from the Instron machine, and Young's modulus calculated from the equation:⁶

$$E = \sigma / \varepsilon \quad (1)$$

where E is the Young's modulus, σ is the stress and ε is the strain.

3. Results and discussion

3.1. Carbon fibre/α-sialon composites without ZrO₂ particles

3.1.1. Sintering of the composites

Temperature is perhaps the key element in successful sintering; not only does it have an effect on densification, but it also influences the reaction between matrix and fibres, and hence subsequent degradation of the fibres. It has been shown⁵ that when 25 wt.% of LAS glass is added, a nearly fully densified α/LAS matrix can be achieved at 1300–1450°C; so in the present study, 25 wt.% of LAS was used. Carbon fibre reinforced α-sialon composites containing relatively high volumes of fibres, (either ~60 vol.% or ~40 vol.% respectively) were first hot-pressed at different temperatures and pressures, and the results are listed in Table 3. As expected, the incorporation of carbon fibres into the α-sialon matrix increased the difficulty of densification, but this appeared to be relatively insensitive to sintering temperature. Because LAS glass softens above 1000°C, below 1450°C there is no obvious reaction and the densification process is actually a kind of 'particle rearrangement' and 'gap filling' by the melt. Therefore, a further increase in temperature only lowers the viscosity of the melt, with no additional liquid formed. However, at higher temperatures (>1550°C), the density of the composites increased to above 96%TD suggesting that a different sintering mechanism had occurred. This might be attributed to reaction between α-sialon, LAS glass and carbon fibre, and this has been confirmed by the fracture behaviour and microstructural analysis.

3.1.2. Fracture behaviour of the composites

Mechanical testing results on carbon fibre reinforced α-sialon composites indicated that the sintering temperature had a strong effect on the mechanical properties (Table 3)

Table 3
Sintering and bending test results for α-sialon composites without ZrO₂ particles

Sample α + C _f	Sintering condition			TD (%)	Strength ^a σ (MPa)	Toughness ^a K _{IC} (MPa m ^{1/2})
	T (°C),	P (MPa),	t (min)			
α + 40 vol.%	1350	15	10	88	189±10	—
α + 40 vol.%	1450	22	10	93	337±20	—
α + 40 vol.%	1550	15	5	89	147±10	—
α + 60 vol.%	1400	15	10	92	165±10	7.3±1.0
α + 60 vol.%	1450	15	10	93	223±20	12.7±2.0
α + 60 vol.%	1500	15	10	92	224±20	9.4±2.0
α + 60 vol.%	1550	15	10	96	93±10	3.6±1.0

^a Mean value of three results.

and fracture behaviour of the composites. Typical load-displacement curves for these samples are given in Fig. 2(a)–(d), and below 1550°C show essentially ‘Class I’ behaviour,¹³ i.e. a characteristic initial matrix cracking stress (arrows in the figure) followed by a region of intermittent cracking with non-linear behaviour until eventual failure at some maximum load followed by a long ‘tail’. Obviously failure is non-catastrophic and the total work of fracture increases considerably above that corresponding to the first matrix crack formation, and thus a high damage tolerance is achieved in these materials. In contrast, material sintered at 1550°C [Fig. 2(d)] shows linear load-displacement behaviour up to a maximum load followed by a sudden decrease in load with very limited continued deformation, indicating that failure was dominated by the propagation of a single dominant crack with only minimal amounts of inelastic strain. The size of the subsequent load reduction is significantly lower than the first matrix cracking load, suggesting that serious degradation of the carbon fibres accompanied by fibre/matrix sticking had occurred at the sintering temperature.

3.1.3. Fracture surfaces

SEM observations of fracture surfaces are shown in Fig. 3(a)–(d) and further confirm the above picture of fracture behaviour. Below 1550°C, it is clear that cracks propagate in a zigzag way, and crack deflection is

clearly observed. Delamination also occurred in samples sintered at low temperatures, which might be an indication of non-uniform distribution of fibres in the matrix caused by weak combinations of different layers. As shown in Fig. 3, all fracture surfaces for the composites hot-pressed below 1550°C demonstrated massive pullout with long fibre lengths exposed.

However, fibre pullout became shorter as the sintering temperature increased, and for example, in composites sintered at 1550°C, the shape of the crack after bend testing [Fig. 3(d)] is completely different. The surface of the crack is smooth, with neither deflection nor delamination observed, and only a few fibres pulled out from the matrix, indicating either a strong frictional force or that some chemical reactions between fibres and matrix had occurred. Preliminary mechanical tests indicated that a significant improvement in fracture toughness was achieved in materials sintered at 1450°C, which gave K_{IC} values as high as 12.7 MPa m^{1/2}. This value is about 3 times that of pure α -sialon ceramics. It is believed that substantial fibre pullout and elastic bridging of the fibres in the crack wake made a significant increase in the fracture toughness. Though these composites exhibited very good fracture toughness, high damage tolerance and non-catastrophic failure, unfortunately, the flexural strength is not satisfactory. It is believed that the low strength is caused partly by degradation and non-homogeneous distribution of the fibres, but mainly

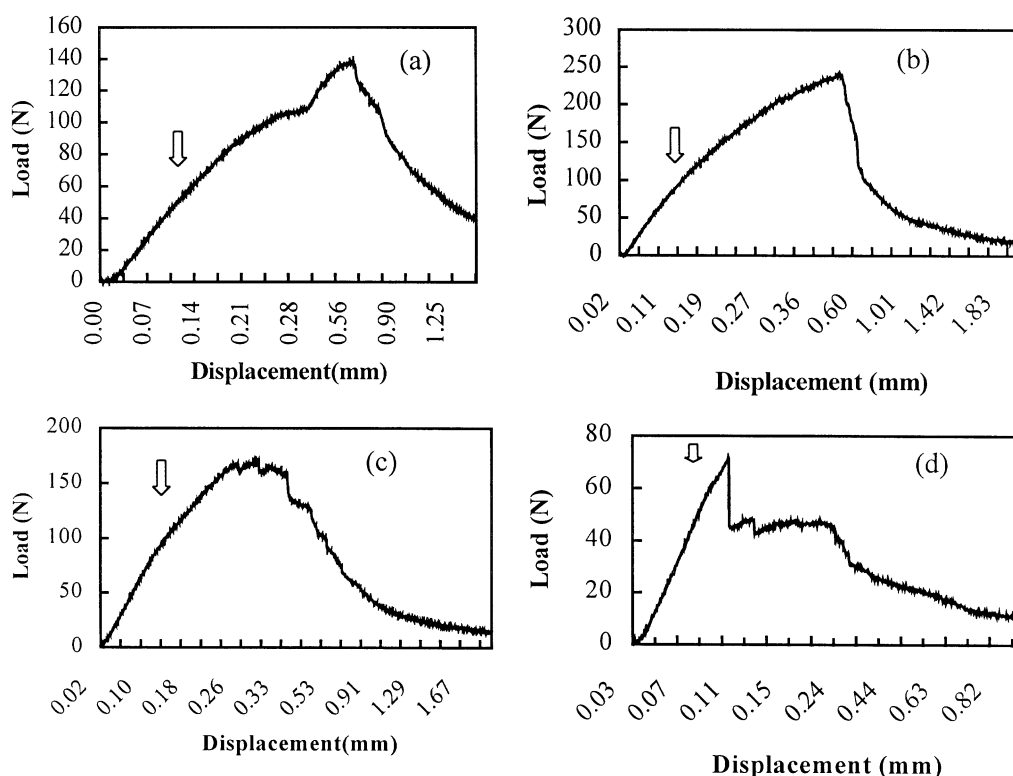


Fig. 2. Load-displacement curves for composites sintered at different temperatures: (a) 1400°C; (b) 1450°C; (c) 1500°C; (d) 1550°C.

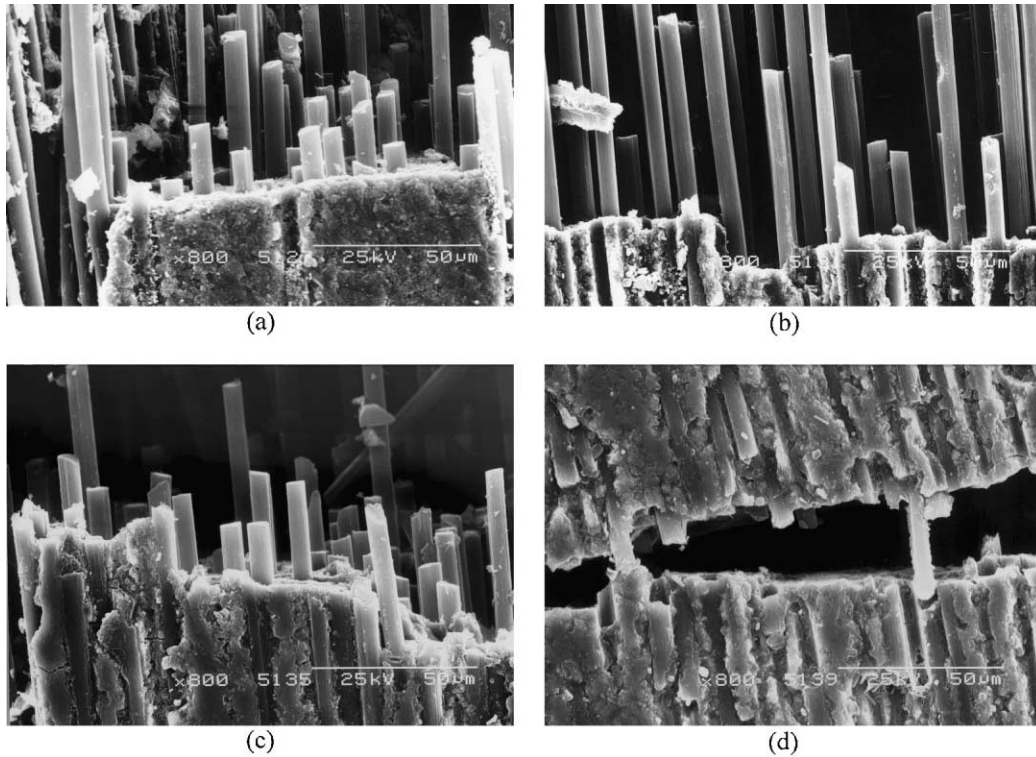


Fig. 3. SEM images of carbon fibre/ α -sialon composites after bend testing. Sintering temperature: (a) 1400°C; (b) 1450°C; (c) 1500°C; (d) 1550°C.

by thermal mismatch between the fibres and the matrix. The latter two reasons both readily cause microcracks in the composites.

3.1.4. Effect of non-uniform distribution of carbon fibres

Our previous work⁵ showed that there is a close relationship between the processing parameters, microstructure and properties of these composites. Many of the properties of fibrous composite materials are strongly dependent on microstructural parameters such as fibre/matrix bonding, and the distribution, volume fraction, alignment and packing arrangement of fibres. If the distribution of the fibres in the composite is not homogeneous, some cracks normal to the fibre directions will be produced because of the difference in thermal expansion coefficients between the fibres and the matrix. In the present work, assuming that the sample is composed of two materials: carbon fibre layers and α /LAS matrix layers, forming alternate sheets with linear thermal expansion coefficients α_f , α_m , elastic moduli, E_f , E_m , and Poisson's ratios ν_f , ν_m , when the composite is cooled from high temperature T_c (the temperature below which the matrix ceases to behave viscoplastically) to room temperature T_r , the temperature difference $\Delta T = T_c - T_r$, will result in thermal expansion changes in the carbon fibres of $\alpha_f \Delta T$ and in the α -sialon matrix of $\alpha_m \Delta T$. These expansions are not the same and the composite must adopt an intermediate overall expansion, determined by the relative elastic moduli and the volume fractions of fibres and matrix, but with the net

compressive force on the carbon fibres equal to the net tensile force in the α -sialon matrix. If σ is this stress, V the volume fraction, and ε the actual strain, then when the composite is cooled down to room temperature, and for a composite in which the continuous fibres are distributed homogeneously:¹⁴

$$\sigma_m V_m + \sigma_f V_f = 0 \quad (2)$$

and therefore

$$\left(\frac{E_m}{1 - \nu_m} \right) (\varepsilon - \varepsilon_m) V_m + \left(\frac{E_f}{1 - \nu_f} \right) (\varepsilon - \varepsilon_f) V_f = 0 \quad (3)$$

Since $V_m + V_f = 1$,

$$\begin{aligned} & \left(\frac{E_m}{1 - \nu_m} \right) (\varepsilon - \varepsilon_m) (1 - V_f) + \left(\frac{E_f}{1 - \nu_f} \right) (\varepsilon - \varepsilon_f) V_f \\ & = 0 \end{aligned} \quad (4)$$

and

$$\begin{aligned} \left(\frac{E_m}{1 - \nu_m} \right) (\varepsilon - \varepsilon_m) &= \left(\frac{E_m}{1 - \nu_m} \right) (\varepsilon - \varepsilon_m) V_f \\ &\quad - \left(\frac{E_f}{1 - \nu_f} \right) (\varepsilon - \varepsilon_f) V_f \end{aligned} \quad (5)$$

In the present study, the Poisson's ratios of the matrix α -sialon and the carbon fibre are similar i.e. $\nu_m \approx \nu_f$, and

so is the difference in strain, i.e. $\varepsilon - \varepsilon_m = \varepsilon - \varepsilon_f = (\alpha_m \Delta T - \alpha_f \Delta T) = \Delta \alpha \Delta T$, where $\Delta \alpha = \alpha_m - \alpha_f$. Therefore, the thermal stress in the matrix can be deduced as:

$$\sigma_m = \left(\frac{E_m - E_f}{1 - \nu_f} \right) \Delta \alpha \Delta T V_f \quad (6)$$

From Eq. (6), the stress caused by thermal mismatch in the matrix is proportional to the volume fraction of the fibres. Therefore, large thermal stresses in some local regions, where the distribution of carbon fibres is not uniform, will result in some cracks in the composite if the stresses are large enough. Therefore, carefully control of the distribution of fibres in the composite is the key to successful fabrication of the composite.

3.1.5. Thermal mismatch in carbon fibre reinforced α -sialon composites

Because the carbon fibres have anisotropic thermal expansion properties, the mismatch between the carbon fibres and the α -sialon matrix should be considered in both the radial and axial directions when carbon fibres are unidirectionally aligned in the composite. The thermal stress caused by thermal expansion difference between the carbon fibres and the matrix in the radial (σ_r) and axial directions (σ_a) can be estimated from the formulae:^{15,16}

$$\sigma_r = \frac{-q E_f E_m [(\alpha_f r - \alpha_m) \Delta T + A/r]}{E_f (1 + \nu_m) + E_m (1 - \nu_f)} \quad (7)$$

$$\sigma_a = (\alpha_m - \alpha_{fa}) \Delta T \frac{E_f V_f}{V_f [(E_f/E_m) - 1] + 1} \quad (8)$$

where ΔT is the temperature change during cooling, q is an adjustable parameter (normally taken as unity), $\alpha_{f,r}$, $\alpha_{f,a}$ are thermal expansion coefficients of the fibres in radial and axial directions and α_m is the matrix thermal expansion coefficient. A is the amplitude of fibre roughness, r is the fibre radius, E_f and E_m are the elastic moduli and ν_f and ν_m are the Poisson's ratios of the fibres and matrix, respectively. In the present system, because the radial thermal expansion coefficient of carbon fibres between room temperature and 900°C is about $8 \times 10^{-6} \text{ } ^\circ\text{C}^{-1}$,^{3,6} which is larger than that of the α matrix ($\sim 5.6 \times 10^{-6} \text{ } ^\circ\text{C}^{-1}$), on cooling, there will be a trend for the carbon fibres to contract away from the matrix; therefore, in the radial direction, the thermal mismatch between fibres and matrix is acceptable. However, in the axial direction, the thermal expansion coefficient of carbon fibre is much smaller than that of the matrix, i.e. $\alpha_{f,a} < \alpha_m$, and cooling from the hot-pressing temperature will put the matrix in tension. In the carbon fibre/ α -sialon system, the magnitude of the tensile strength can be calculated by substituting values of $E_f = 257 \text{ GPa}$, $E_m = 142 \text{ GPa}$, $\alpha_{f,a} \approx 0$, $\alpha_m \approx 5.6 \times 10^{-6} \text{ } ^\circ\text{C}^{-1}$, $\Delta T = 1000^\circ\text{C}$ into Eq.

(11), and the calculated tensile stress in the matrix is about 466 MPa for a composite containing 40% of carbon fibres and $\sim 700 \text{ MPa}$ for a composite containing 60 vol.% of carbon fibres. This is greater than the strength of the matrix. Therefore, the thermal mismatch between the carbon fibres and the matrix together with non-homogeneous distribution of the fibres results in transverse microcracks in the matrix as shown in Fig. 4.

3.2. Carbon fibre/ α -sialon composites with ZrO_2 particles

3.2.1. Elimination of cracks

The introduction of ZrO_2 into ceramics was originally developed to improve the fracture toughness by $t \rightarrow m$ ZrO_2 transformation. Accompanying this transformation, there is about a 3–5% volume increase, and this can also be used to make compensation for the volume contraction of the matrix during cooling. Addition of ZrO_2 to a silicon nitride or oxynitride matrix has been explored and shown to be a promising route for eliminating microcracking in carbon fibre reinforced composites.^{3, 4}

Guo et al.³ reported that cracks perpendicular to the fibres disappeared with a 1 wt.% ZrO_2 addition, but it was better to use a 5 wt.% ZrO_2 addition according to their results. Zhang and Thompson⁴ showed that when less than 20 wt.% ZrO_2 is added to a nitrogen glass matrix, cracks still occur, but the number of cracks is reduced compared with ZrO_2 -free materials. Actually the amount of ZrO_2 needed is dependent on the volume of carbon fibres in the composite, the thermal expansion coefficient of the matrix, and the chemical compatibility between the matrix and ZrO_2 , the latter effect being very important, as will be discussed later. In the present carbon fibre reinforced α -sialon samples, when 5 wt.% of ZrO_2 was added, cracks still occurred; however, when 20 wt.% ZrO_2 was added, all microcracks had disappeared. Polished sections of composites containing 20 wt.% ZrO_2 were examined by SEM, and Fig. 5 shows

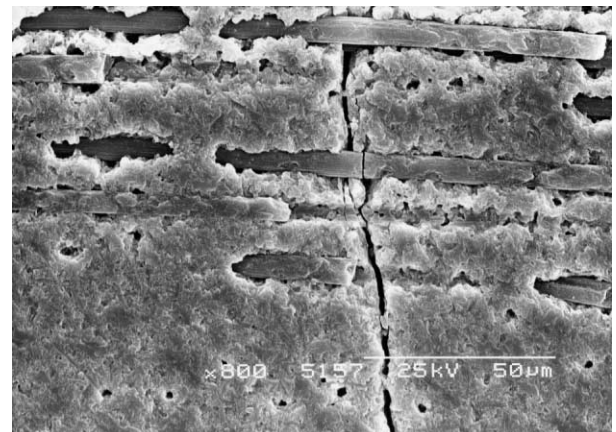


Fig. 4. Microcracking in carbon fibre/Li- α -sialon composites.

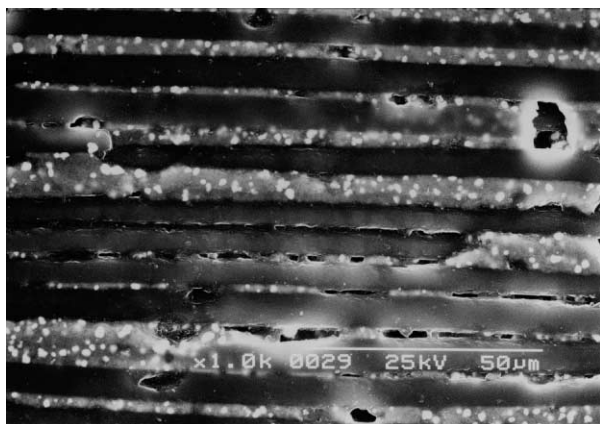


Fig. 5. Polished section of carbon fibre/ α -sialon/ ZrO_2 composites parallel to the fibre direction (back-scattered electron image).

sections parallel to the fibre direction in these materials. It can be seen that all the microcracks have been eliminated when 20 wt.% of ZrO_2 is incorporated suggesting that this is an effective way of controlling cracking in these composites. As expected, when the cracks were eliminated, the strength of the samples was significantly improved (Fig. 6). The bending strength for carbon fibre reinforced α -sialons containing 20 wt.% ZrO_2 reached a value of ~ 410 MPa, with a fracture toughness of ~ 12 MPa $\text{m}^{1/2}$. It is believed that the addition of ZrO_2 eliminated cracks in the matrix so that the external load was effectively transferred to the high strength, high elastic and high strain carbon fibres, thus promoting successful toughening.

3.2.2. Compatibility between ZrO_2 and an α -sialon matrix

The chemical compatibility of ZrO_2 with a nitride matrix should be carefully considered because $t \rightarrow m$ transformation may not occur if ZrO_2 reacts with the matrix to form ZrN , zirconium oxynitride or nitrogen stabilised ZrO_2 ,^{17–20} especially when fine ZrO_2 particles are used. These compounds have tetragonal or cubic structures, structurally similar to t - or c - ZrO_2 but do not undergo normal transformation; moreover, just as ZrN , they are easily oxidised into m - ZrO_2 in air at low temperatures (600–800°C) resulting in a large volume increase and stress build-up. This cannot occur in ZrO_2 -toughened oxide ceramics, however, the volume increase resulting from the formation of m - ZrO_2 by oxidation here could improve the fracture toughness by generating surface stress within the material which then opposes crack growth;¹⁸ in the present work, it is believed that the volume increase is mainly from the normal $t \rightarrow m$ transformation, even though from Fig. 7, it can be seen that small amounts of the rhombohedral zirconium oxynitride $\text{Zr}_7\text{O}_8\text{N}_4$ formed together with $\text{Si}_2\text{N}_2\text{O}$ in the samples suggesting that some of the ZrO_2 had reacted with the Li- α -sialon matrix. These two phases have very

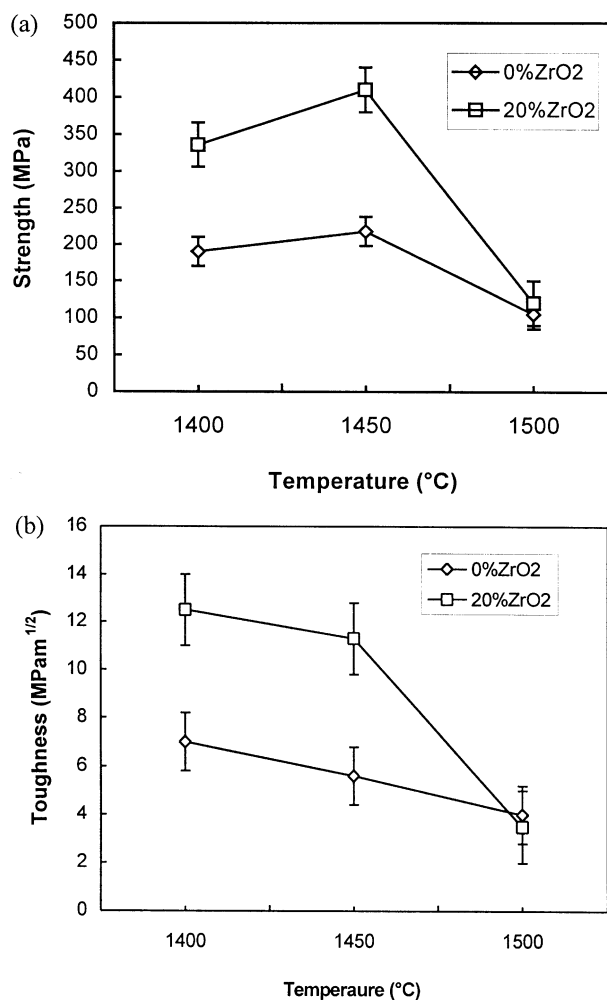
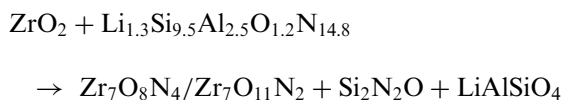


Fig. 6. The bending strength (a) and fracture toughness (b) of carbon fibre reinforced α -sialon composites prepared at different temperatures ($V_f = 40\%$).

similar reflections except in the small angle region, so it is not easy to distinguish them using conventional XRD methods.²⁰ The reaction between ZrO_2 and α -sialon is believed to occur qualitatively as follows:



Full details of the reaction mechanism between ZrO_2 and α -sialon needs further study.

In these experiments, it is believed that the introduction of ZrO_2 played an important role in changing the thermal behaviour of the composite. When the sample was cooled down from the sintering temperature to a temperature of $\sim 1170^\circ\text{C}$, i.e. the normal $t \rightarrow m$ ZrO_2 phase transformation temperature, tetragonal ZrO_2 started to transform into monoclinic ZrO_2 . However, whether the $t \rightarrow m$ ZrO_2 phase transformation does occur or not is determined by various factors, such as

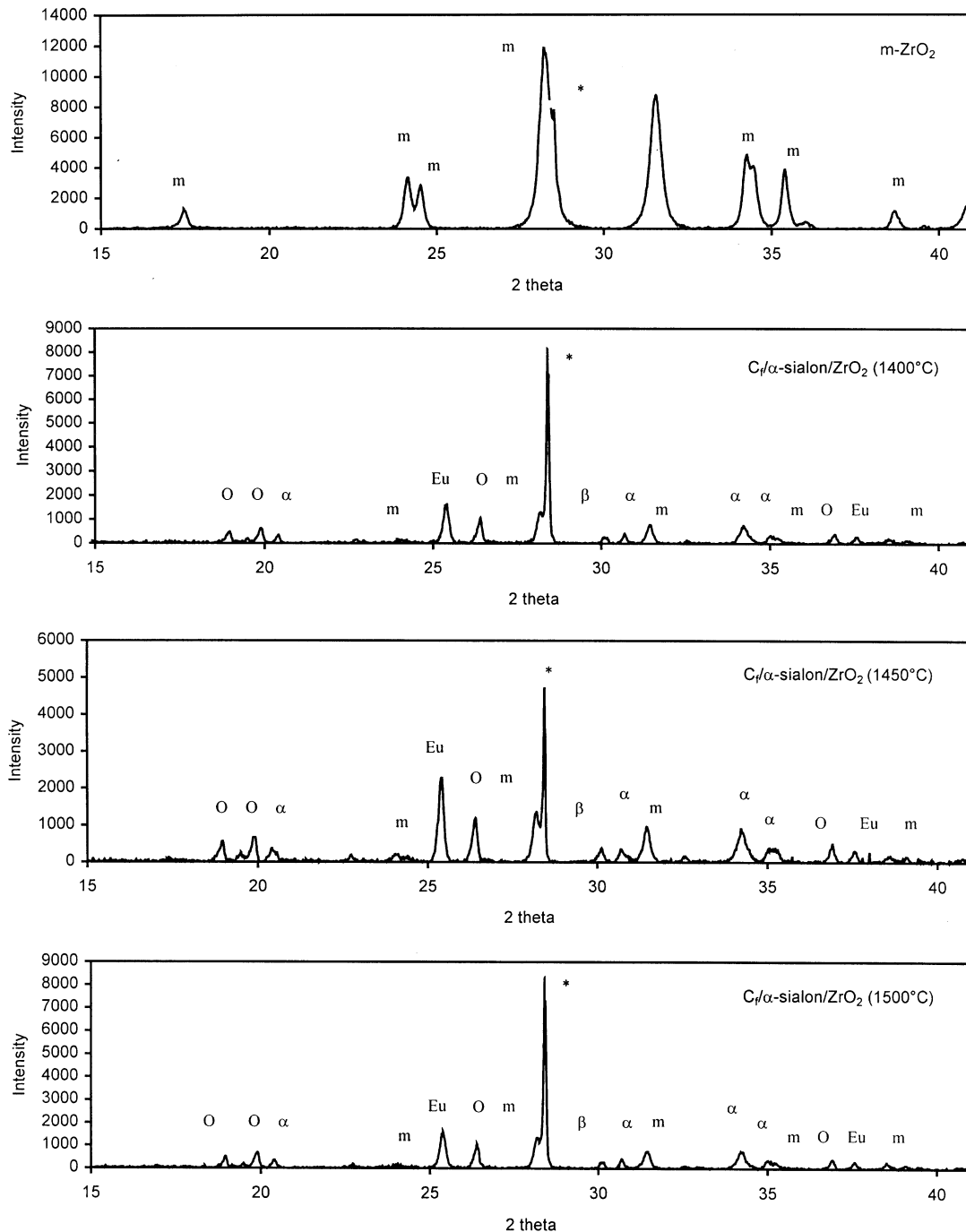


Fig. 7. XRD results of the ZrO_2 powder and $\text{C}_f/\alpha\text{-sialon}/\text{ZrO}_2$ composites sintered at different temperatures. *: Si; m: $m\text{-ZrO}_2$; α : $\alpha\text{-sialon}$; β : $\text{Zr}_7\text{O}_8\text{N}_4/\text{Zr}_7\text{O}_{11}\text{N}_2$; Eu: eucryptite; O: $\text{Si}_2\text{N}_2\text{O}$.

the particle size of ZrO_2 , the chemical composition and the local stress situation, with the transformation temperature decreasing with the size of the dispersed ZrO_2 particles. Large $t\text{-ZrO}_2$ particles will easily undergo transformation to $m\text{-ZrO}_2$ at higher temperatures. Actually the transformation does not take place at a fixed temperature but over a temperature range. Fine-grained ZrO_2 will transform to $m\text{-ZrO}_2$ at temperatures much lower than 1170°C and therefore, the particle size of the ZrO_2 used is important. If coarse-grained ZrO_2 is

used, any ZrO_2 present in the unstabilised tetragonal form after hot-pressing will spontaneously transform into the monoclinic form on cooling immediately below $\sim 1170^\circ\text{C}$. At this temperature, although most of the $\alpha\text{-sialon}$ matrix is hard, the LAS glass is still soft so the volume increase arising from $t \rightarrow m$ transformation is partly absorbed by glass deformation; this is especially marked in the case of the pure glass matrix. In this work, a very fine monoclinic ZrO_2 powder with crystallite size ~ 27 nm was used to reduce the $t \rightarrow m$ transformation

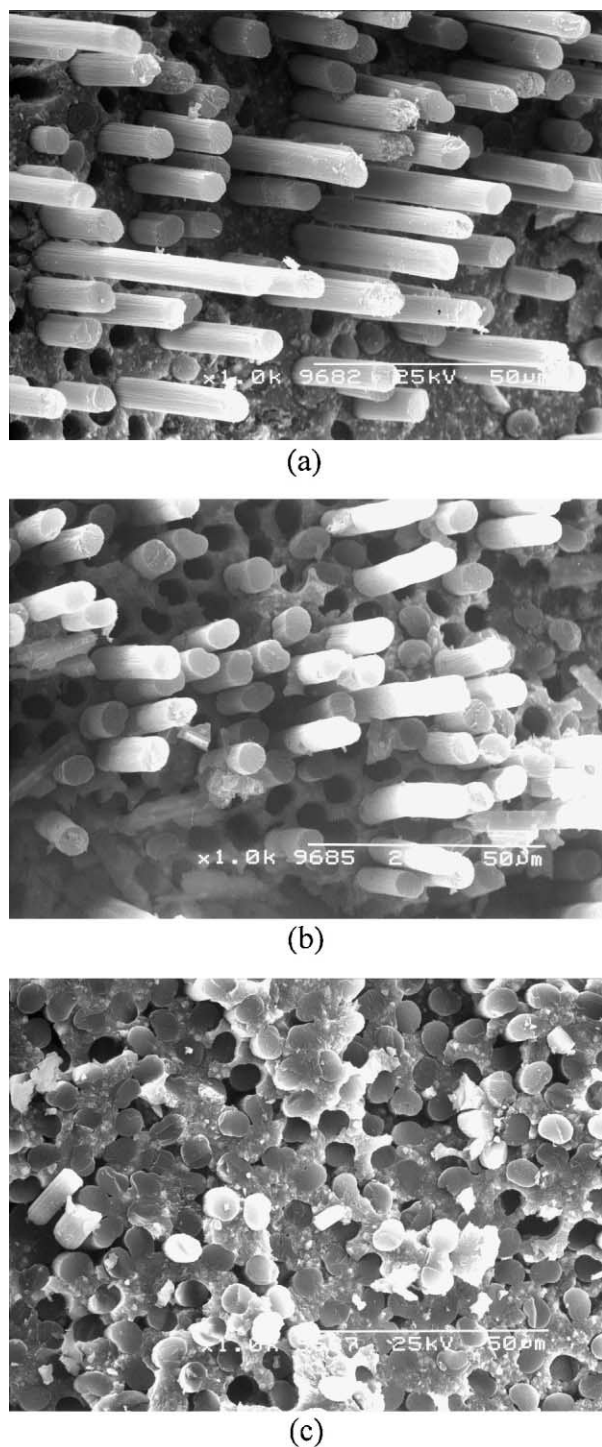


Fig. 8. Fracture surfaces of carbon fibre and ZrO_2 particle reinforced α -sialon composites prepared at (a) 1400°C, (b) 1450°C and (c) 1500°C; magnifications all 1 k.

temperature. To ensure that the $t \rightarrow m$ transformation occurs immediately below the softening temperature, the thermal expansion coefficient compatibility between the matrix and the ZrO_2 must also be considered. If the ZrO_2 particles are under such a high compressive pressure that the $t \rightarrow m$ transformation cannot occur, the added ZrO_2 will not perform its role satisfactorily. Ide-

ally, the difference in thermal expansion coefficients between the dispersed ZrO_2 phase (α_p) and the matrix (α_m) should be small to keep the matrix and the ZrO_2 particles suitably bonded during cooling on the one hand, whilst still ensuring that the $t \rightarrow m$ transformation occurs. In the α -sialon/ ZrO_2 matrix, $\Delta\alpha = \alpha_{\text{ZrO}_2} - \alpha_{\text{sialon}} > 0$, so, the constraint on ZrO_2 particles from the matrix is small on cooling, and therefore t - ZrO_2 tends to transform to m - ZrO_2 . X-ray diffraction analysis (Fig. 7) indicated that most of the ZrO_2 in the composites was in the monoclinic form at room temperature, confirming that the martensitic phase transformation had taken place during cooling. When this phase transformation takes place, tensile stresses in the matrix due to the thermal mismatch between the fibres and matrix are reduced, and the volume expansion of 3–5% arising from $t \rightarrow m$ transformation makes some compensation for the volume contraction of the matrix, and when the volume of ZrO_2 reaches a certain content, microcracks in the matrix can be completely eliminated. It should be pointed out that if too much ZrO_2 is added, excessive compressive stresses will be built up on the carbon fibres, making it difficult for the fibres to be pulled out. From the fracture surface of the composites sintered at different temperatures (Fig. 8), it can be seen that a high fibre pullout density with long pullout lengths was observed on fracture surfaces below 1500°C; however, when the temperature was increased to 1500°C, the fracture surface is quite smooth, and there is very limited fibre pullout suggesting that chemical reactions have occurred between the fibres and the matrix during sintering. The load-displacement curves (Fig. 9) indicated that failure took place by delamination, with cracks appearing progressively in a controlled manner rather than in the catastrophic manner observed in monolithic α -sialon ceramics at low temperatures ($< 1500^\circ\text{C}$) as reported previously.⁵ It can be seen from Fig. 9(a) and (b), that at the beginning of the test, the composites extended elastically, the displacement being directly proportional to the load. Beyond the elastic limit, the applied load produced plastic deformation until the maximum load was reached, at which stage the fibres were broken; then the load dropped with increasing displacement forming a long tail during which time the fibres were pulled out suggesting these composites have a high damage tolerance. In the present work, the toughening effect mainly comes from the carbon fibres, but the introduction of monoclinic ZrO_2 provides an excellent method of overcoming thermal mismatch between the carbon fibres and the α -sialon matrix, eliminating micro-cracks and hence improving the strength. Therefore, a synergistic role of toughening and strengthening in the composites has been achieved. For this to take place, all factors affecting the transformability of ZrO_2 particles in the matrix have to be carefully controlled.

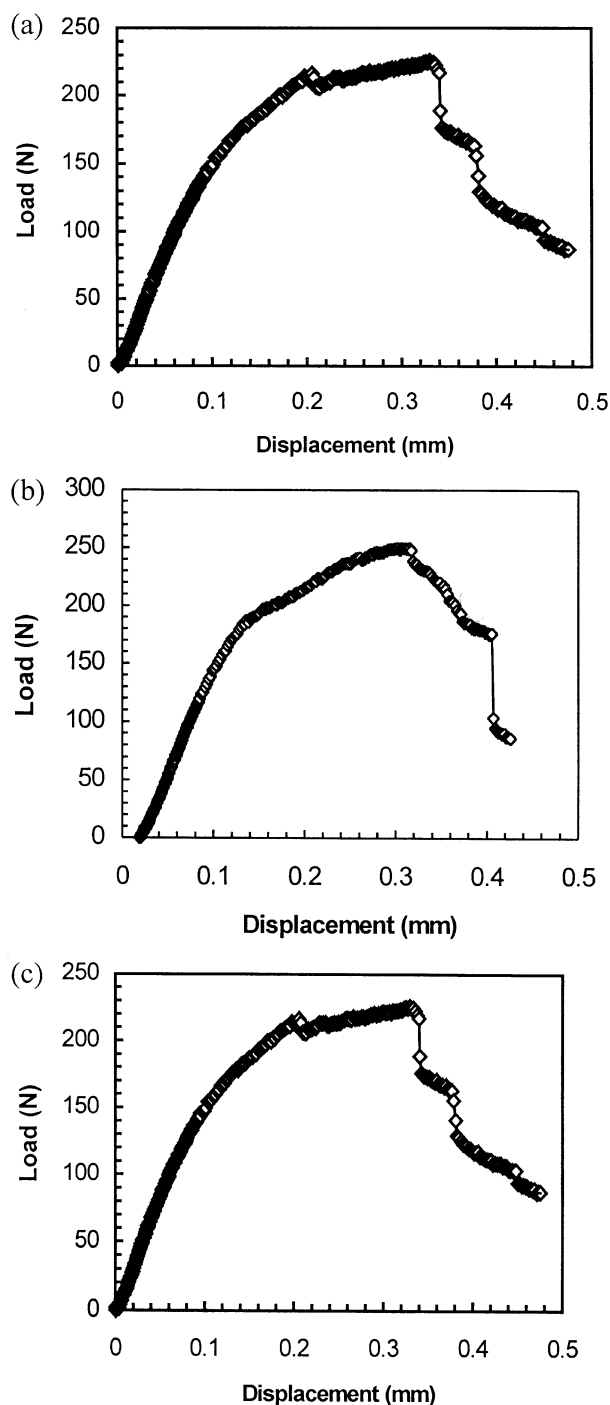


Fig. 9. Load-displacement curves for carbon fibre and ZrO_2 particle reinforced α -sialon composites prepared at (a) 1400°C, (b) 1450°C, (c) 1500°C.

4. Conclusions

(1) In ZrO_2 free samples, the larger radial thermal expansion of the carbon fibres is believed to be important in creating a suitable interface between fibre and matrix. This interface results in a tough non-brittle fracture behaviour; on the other hand, the near-zero axial thermal expansion of the carbon fibres induces a

large tensile stress and causes some cracks in the matrix during cooling. The degradation of the fibres and microcracks in the composites are the main reasons for the relatively low flexural strength measured.

(2) By introducing 20 wt.% of monoclinic ZrO_2 particles into the starting mix, cracks in the matrix were totally eliminated by the volume increase associated with the $t \rightarrow m$ ZrO_2 transformation. As a result, the mechanical properties of these materials were noticeably improved compared with ZrO_2 -free samples and a simultaneous strengthening and toughening effect achieved.

Acknowledgements

The authors would like to thank the Defence Evaluation and Research Agency (DERA) for financial support.

References

1. Levitt, S. R., High-strength graphite fibre/lithium aluminosilicate composites. *J. Mater. Sci.*, 1973, **8**, 793–806.
2. Nakano, K., Carbon fibre reinforced ceramic composites. *J. Adv. Sci.*, 1990, **2**(4), 247–256.
3. Guo J. K., Mao, Z., Bao, C., Wang, T. and Yan, D. S., Carbon fibre reinforced silicon nitride composite. *J. Mater. Sci.*, 1982, 3611–3316.
4. Zhang, E. and Thompson, D. P., Carbon fibre reinforcement of nitrogen glass. *Composites Part A*, 1997, **28A**, 581–586.
5. Yu, Z. B. and Thompson, D. P., Fabrication and mechanical behaviour of carbon fibre reinforced alpha sialon composites, FRC'98, 15–17 April. In: *Proceeding of the Seventh International Conference on Fibre Reinforced Composites, Consolidating New Applications*, ed A. G. Gibson. Woodhead Publishing Limited, 1998, pp. 264–270.
6. Richerson, D. W., *Modern Ceramics Engineering: Properties, Processing and Use in Design*. Marcel DEKKER, New York, 1992.
7. Guo, J. K. and Zhu, P. N., Design principles of multiphase ceramic materials. *J. Chinese Ceram. Soc.*, 1996, **24**(1), 7–12.
8. Zhang, E., Liddell, K. and Thompson, D. P., Glass forming regions and thermal expansion of some Ln-Si-Al-O-N glasses ($\text{Ln} = \text{La, Nd}$). *Br. Ceram. Trans.*, 1996, **95**(4), 169–172.
9. Yu, Z. B., Thompson, D. P. and Bhatti, A. R., Preparation of single phase $\text{Li-}\alpha$ -sialon ceramics. *Br. Ceram. Trans.*, 1998, **97**(2), 41–47.
10. Levitt, S. R., High-strength graphite-fibre/lithium aluminosilicate composites. *J. Mater. Sci.*, 1973, **8**, 793–806.
11. Sambell, R. A. J., Briggs, A., Phillips, D. C. and Bowen, D. H., Carbon fibre composites with ceramic and glass matrices. *J. Mater. Sci.*, 1972, **7**, 676–681.
12. *Phase Diagrams for Ceramists*, ed. E. M. Levin, E. R. Robbins and H. F. McMurdie. *J. Am. Ceram. Soc.*, 1964.
13. Evans, A. G., Zok, F. W. and Davis, J., The role of interfaces in fibre-reinforced brittle matrix composites. *Composites Science and Technology*, 1991, **42**, 3–24.
14. Kingery, W. D., Bowen, H. K., Uhlmann, D. R. *Introduction to Ceramics*, 2nd. edn. Wiley-Interscience, New York, 1976.
15. Chawla, K. K., *Ceramic Matrix Composites*. Chapman & Hall, 1993.
16. Kerans, R. J. and Parthasarathy, T. A., Theoretical analysis of the fibre pullout and push out test. *J. Am. Ceram. Soc.*, 1991, **74**(7), 1585–1596.

17. Claussen, N., Wagner, R., Gauckler, L. J. and Petzow, G., Nitride-stabilized cubic zirconia. *J. Am. Ceram. Soc.*, 1978, **7–8**, 369–376.
18. Lange, F. F., Compressive surface stresses developed in ceramics by an oxidation induced phase change. *J. Am. Ceram. Soc.*, 1980, **63**(1–2), 38–40.
19. Cheng Yi-Bing and Thompson, D. P., Nitrogen containing tetragonal zirconia. *J. Am. Ceram. Soc.*, 1991, **74**(5), 1135–1138.
20. Lerch, M., Nitridation of zirconia. *J. Am. Ceram. Soc.*, 1996, **79**(10), 2641–2644.